Thermodynamic and Kinetic Studies on the Binding of Nitric Oxide to a New Enzyme Mimic of Cytochrome P450

Alicja Franke,[†] Natalya Hessenauer-Ilicheva,[†] Dominik Meyer,[‡] Grażyna Stochel,[§] Wolf-D. Woggon,*[,‡] and Rudi van Eldik*[,†]

Contribution from the Institute for Inorganic Chemistry, University of Erlangen-Nürnberg, Egerlandstrasse 1, 91058 Erlangen, Germany, Department of Chemistry, University of Basel, St. Johanns-Ring 19, 4056 Basel, Switzerland, and Faculty of Chemistry, Jagiellonian University, Ingardena 3, 30 060 Kraków, Poland.

Received February 4, 2006; E-mail: vaneldik@chemie.uni-erlangen.de

Abstract: A new model for the P450 enzyme carrying a SO_3^- ligand coordinated to iron(III) (complex **2**) reversibly binds NO to yield the nitrosyl adduct. The rate constant for NO binding to **2** in toluene is of the same order of magnitude as that found for the nitrosylation of the native, substrate-bound form of $P450_{cam}$ ($E\cdot S\text{-}P450_{cam}$). Large and negative activation entropy and activation volume values for the binding of NO to complex **2** support a mechanism that is dominated by bond formation with concomitant iron spin change from $S = ^5/_2$ to $S = 0$, as proposed for the reaction between NO and $E\cdot S\text{-}P450_{cam}$. In contrast, the dissociation of NO from **2**(NO) was found to be several orders of magnitude faster than the corresponding reaction for the $E\cdot S\text{-}P450_{cam}$/NO system. In a coordinating solvent such as methanol, the alcohol coordinates to iron-(III) of **2** at the distal position, generating a six-coordinate, high-spin species **5**. The reaction of NO with **5** in methanol was found to be much slower in comparison to the nitrosylation reaction of **2** in toluene. This behavior can be explained in terms of a mechanism in which methanol must be displaced during Fe−NO bond formation. The thermodynamic and kinetic data for NO binding to the new model complexes of P450 (**2** and **5**) are discussed in reference to earlier results obtained for closely related nitrosylation reactions of cytochrome $P450_{cam}$ (in the presence and in the absence of the substrate) and a thiolate-ligated iron(III) model complex.

Introduction

Synthetic iron porphyrins have received considerable attention from many groups, in particular regarding their use as chemical models in a variety of enzymatic oxidations such as those catalyzed by cytochromes P450, catalases, and peroxidases.[1] It was shown that the nature of the anionic proximal ligand coordinating to iron plays a crucial role in controlling the properties and reactivity of the heme model complexes in such catalytic processes.[2] In this context, heme−thiolate proteins like cytochromes P450 are of particular interest due to the significance of the quite unusual thiolate ligand with respect to spin-

state equilibria of the resting state, redox potential of the iron porphyrin, and the electronic nature of the high-valent iron(IV) oxo intermediate. Consequently, over the past three decades, many groups have focused their efforts on the synthesis of thiolate-ligated iron porphyrins in order to understand the function of the thiolate ligand and to mimic P450 reactivity.[3−5] Although a number of sophisticated iron(III) porphyrin−thiolate complexes were synthesized, most of them remained structural models of the active site, displaying significant differences from

[†] University of Erlangen-Nürnberg.
[‡] University of Basel.
[§] Jagiellonian University.

(1) (a) Watanabe, Y. In *The Porphyrin Handbook*; Kadish, K. M., Smith, K. M., Guilard, R., Eds.; Academic: New York, 2000; Vol. 4, Chapter 30, pp 97−117. (b) McLain, J. L.; Lee, J.; Groves, J. T. In *Biomimetic Oxidations Catalyzed by Transition Metal Complexes*; Meunier, B., Ed.; Imperial College Press: London, 2000, pp 91−169. (c) Montanari, F.; Cassela, L. *Metalloporphyrins Catalyzed Oxidations*; Kluwer Academic Publishers: Dordrecht, The Netherlands, 1994. (d) Traylor, T. G.; Traylor, P. S. In *Active Oxygen in Biochemistry*; Valentine, J. S., Foote, C. S., Greenberg, A., Liebman, J. F., Eds.; Blackie Academic and Professional, Chapman and Hall: London, 1995; pp 84−187. (e) Ingold, K. U.; MacFaul, P. A. In *Biomimetic Oxidations Catalyzed by Transition Metal Complexes*; Meunier, B., Ed.; Imperial College Press: London, 2000; pp 45−89. (f) Meunier, B. *Chem. Rev.* **1992**, *92*, 1411.
(2) (a) Dawson, J. H. *Science* **1988**, *240*, 433. (b) Poulus, T. L. *J. Biol. Inorg. Chem.* **1996**, *1*, 356. (c) Goodin, D. B. *J. Biol. Inorg. Chem.* **1996**, *1*, 360. (d) Franzen, S.; Roach, M. P.; Chen, Y.-P.; Dyer, R. B.; Woodruff, W. H.; Dawson, J. H. *J. Am. Chem. Soc.* **1998**, *120*, 4658.

(3) (a) Aissaoui, H.; Ghirlanda, S.; Gmür, C.; Woggon, W.-D. *J. Mol. Catal. A: Chem.* **1996**, *113*, 393. (b) Aissaoui, H.; Bachmann, R.; Schweiger, A.; Woggon, W.-D. *Angew. Chem., Int. Ed.* **1998**, *37*, 2998. (c) Woggon, W.-D.; Wagenknecht, H.-A.; Claude, C. *J. Inorg. Biochem.* **2001**, *83*, 289. (d) Lochner, M.; Meuwly, M.; Woggon, W.-D. *Chem. Commun.* **2003**, 1330. (e) Lochner, M.; Mu, L.; Woggon, W.-D. *Adv. Synth. Catal.* **2003**, *345*, 743.
(4) (a) Higuchi, T.; Uzu, S.; Hirobe, M. *J. Am. Chem. Soc.* **1990**, *112*, 7051. (b) Higuchi, T.; Shimada, K.; Maruyama, N.; Hirobe, M. *J. Am. Chem. Soc.* **1993**, *115*, 7551. (c) Higuchi, T.; Hirobe, M. *J. Mol. Catal. A: Chem.* **1996**, *113*, 403. (d) Urano, Y.; Higuchi, T.; Hirobe, M.; Nagano, T. *J. Am. Chem. Soc.* **1997**, *119*, 12008. (e) Ohno, T.; Suzuki, N.; Dokoh, T.; Urano, Y.; Kikuchi, K.; Hirobe, M.; Higuchi, T.; Nagano, T. *J. Inorg. Biochem.* **2000**, *82*, 123. (f) Dokoh, T.; Suzuki, N.; Higuchi, T.; Urano, Y.; Kikuchi, K.; Nagano, T. *J. Inorg. Biochem.* **2000**, *82*, 127. (g) Suzuki, N.; Higuchi, T.; Nagano, T. *J. Am. Chem. Soc.* **2002**, *124*, 9622. (h) Suzuki, N.; Higuchi, T.; Urano, Y.; Kikuchi, K.; Uekusa, H.; Ohashi, Y.; Kitagawa, T.; Nagano, T. *J. Am. Chem. Soc.* **1999**, *121*, 11571.
(5) (a) Matsu-ura, M.; Tani, F.; Nakayama, S.; Nakamura, N.; Naruta, Y. *Angew. Chem., Int. Ed.* **1989**, *2000*, 39. (b) Tani, F.; Matsu-ura, M.; Nakayama, S.; Ichimura, M.; Nakamura, N.; Naruta, Y. *J. Am. Chem. Soc.* **2001**, *123*, 1133. (c) Tani, F.; Matsu-ura, M.; Nakayama, S.; Naruta, Y. *Coord. Chem. Rev.* **2002**, *226*, 219. (d) Matsu-ura, M.; Tani, F.; Naruta, Y. *J. Am. Chem. Soc.* **1941**, *2002*, 124.
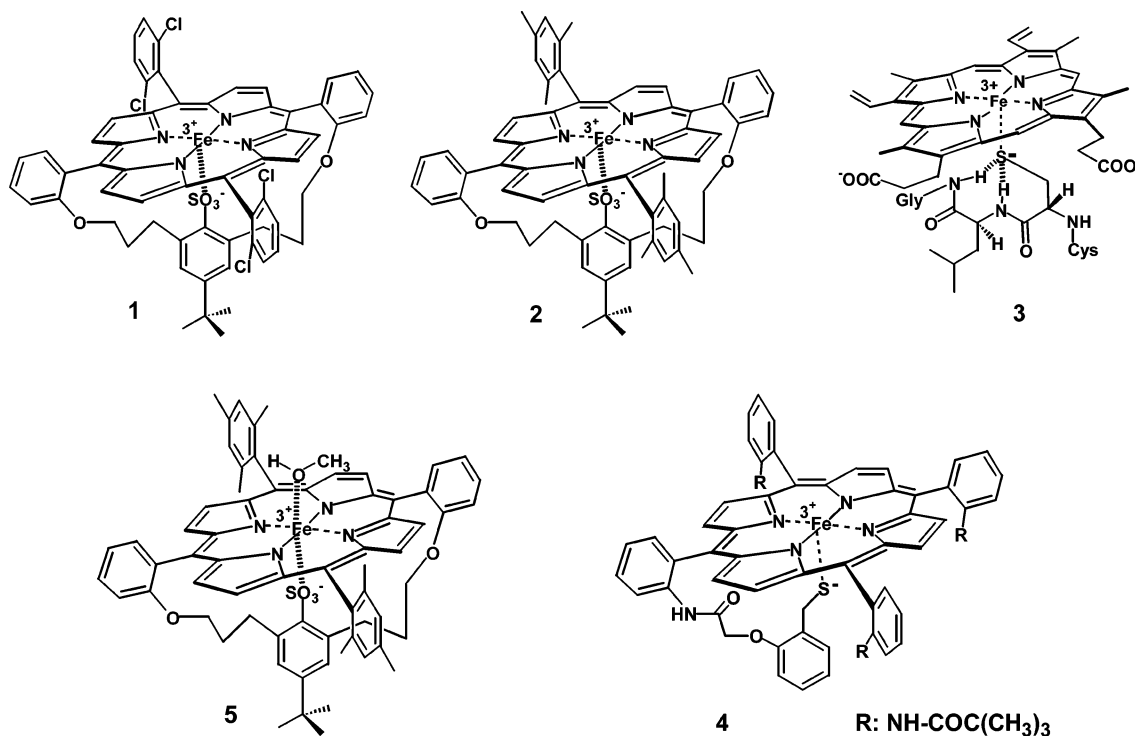
Figure 1. P450 enzyme models (**1** and **2**[7], **4**[4]) and coordination sphere of P450$_{cam}$ (**3**).

P450 enzymes regarding redox potentials and spin-state equilibria of the iron(III) resting state.[6] Furthermore, most of these approaches failed to provide oxidation catalysts with decent turnover, which could be attributed to the instability of both the porphyrin chromophore and the thiolate ligand in the presence of strong oxidants such as PhIO, mCPBA, and H_2O_2 which are usually employed in the "shunt" pathway.[7]

To find more suitable enzyme mimics, the Woggon group has synthesized two new complexes, **1** and **2** (Figure 1), in which the RS$^-$ ligand is replaced by a RSO$_3^-$ group.[8] The SO$_3^-$ group has been introduced because DFT calculations revealed that ca. 40% of a negative charge is localized at the oxygen that coordinates to iron.[8d] Thus, it seemed reasonable that such a system would mimic the coordination sphere of several native P450's, such as P450$_{cam}$, P450$_{terp}$, P450$_{eryF}$, and P450$_{BM-3}$, which display hydrogen bonding of the thiolate ligand to two amino acids of the protein backbone (see **3**, Figure 1). This concept was confirmed by several experiments. For example, **1** and **2** show redox potentials E_o = −210 and −290 mV, respectively (vs SCE measured in 0.1 M LiClO$_4$, LiBr saturated DMF with ferrocene as an internal standard),[8b] indicating that exchanging the thiolate for SO$_3^-$ ligand causes an anodic shift of ca. 300 mV.[3] The E_o value of **2** is close to that obtained with a model compound that has two hydrogen bonds to a

thiolate coordinating to iron (E_o = −350 mV vs SCE in CH$_2$-Cl$_2$)[9] and is also similar to the redox potential determined for the E·S complex of P450$_{cam}$ (E_o = −170 mV vs NHE, which is equivalent to −411 mV vs SCE). However, it should be kept in mind that E_o depends very much on the selected solvent and counterion. Hence, it is not possible to interpret a difference of 20−50 mV between model and native systems in more detail.

Further DFT calculation predicted, and X-ray structures confirmed, the coordination of one oxygen of the SO$_3^-$ group to Fe(III).[8d,f] Complexes **1** and **2** were fully characterized by UV−vis, EPR, and ESI-MS spectroscopy, and in particular the more reactive, electron-deficient *meso*-dichlorophenyl-substituted porphyrin **1** displayed a rather broad spectrum of P450-type reactions such as epoxidation, N-dealkylation, cleavage of diols, and hydroxylation of nonactivated C−H bonds.[8e,f] Preliminary UV−vis experiments also revealed that the oxo iron-(IV) porphyrin radical cation can be produced from **2**.[8f] The main practical advantage of **1** and **2**, as compared to corresponding model complexes with a thiolate ligand, is the inertness of the SO$_3^-$ ligand toward oxidation and *S*-nitrosation.

In efforts to improve the mechanistic understanding of the catalytic action of cytochrome P450 and the essence of its biological functions, we have focused on the dynamics of NO interaction with the iron(III) heme−thiolate centers. It is known that NO binding to the catalytic site of enzymes such as nitric oxide reductase (P450$_{nor}$),[10a,b] nitric oxide synthase (NOS),[10c−f] and nitrophorins from *Cimex lectularius* (NO transport heme−

(6) Woggon, W.-D. *Chimia* **2001**, *55* (4), 366.
(7) (a) Tang, S. C.; Koch, S.; Papaefthymiou, G. C.; Foner, S.; Frankel, R. B.; Ibers, J. A.; Holm, R. H. *J. Am. Chem. Soc.* **1976**, *98*, 2414. (b) Caron, C.; Mitschler, A.; Riviere, G.; Ricard, L.; Schapacher, M.; Weiss, R. *J. Am. Chem. Soc.* **1979**, *101*, 7401. (c) Ogoshi, H.; Sugimoto, H.; Yoshida, Z. *Tetrahedron Lett.* **1975**, *27*, 2289.
(8) (a) Woggon, W.-D.; Leifels, T.; Sbaragli, L. *Cytochromes P450: Biochemistry, Biophysics and Drug Metabolism*; Presented at the 13th International Conference on Cytochromes P450, Prague, Czech Republic, June 29−July 3, 2005. (b) Meyer, D. N.; Woggon, W. -D. *Chimia* **2005**, *59* (3), 85. (c) Woggon, W.-D. *Acc. Chem. Res.* **2005**, *38*, 127. (d) Kozuch, S.; Leifels, T.; Meyer, D.; Sbaragli, L.; Shaik, S.; Woggon, W.-D. *Synlett.* **2005**, *4*, 675. (e) Sbaragli, L.; Woggon, W.-D. *Synthesis* **2005**, *9*, 1538. (f) Meyer, D.; Leifels, T.; Sbaragli, L.; Woggon, W.-D. *Biochem. Biophys. Res. Commun.* **2005**, *338*, 372.

(9) Ueyama, N.; Nishikawa, N.; Yamada, Y.; Okamura, T.; Nakamura, A. *J. Am. Chem. Soc.* **1996**, *118*, 12826−12827.
(10) (a) Shimizu, H.; Obayashi, E.; Gomi, Y.; Arakawa, H.; Park, S.-Y.; Nakamura, H.; Adachi, S.; Shoun, H.; Shiro, Y. *J. Biol. Chem.* **2000**, *275*, 4816. (b) Obayashi, E.; Takahashi, S.; Shiro, Y. *J. Am. Chem. Soc.* **1998**, *120*, 12964. (c) Hurshman, A. R.; Marletta, A. *Biochemistry* **1995**, *34*, 5627. (d) Abu-Soud, H. M.; Wang, J.; Rousseau, D. L.; Fukuto, J. M.; Ignarro, L. J.; Stuehr, D. J. *J. Biol. Chem.* **1995**, *270*, 22997. (e) Couture, M.; Adak, S.; Stuehr, D. J.; Rousseau, L. *J. Biol. Chem.* **2001**, *276*, 38280.

thiolate proteins from the bedbug)[11] is essential for their biological function. In this context, an earlier report from the Erlangen/Krakow laboratories focused on the reaction of NO with native cytochrome P450$_{cam}$ and revealed mechanistic details on the reversible binding of NO to P450$_{cam}$ in the absence and in the presence of the substrate (+)-camphor.[12] Very recently, these groups studied NO binding to the synthetic heme–thiolate complex **4**,[4] which was considered as a reasonable model for the kinetics of the analogous reactions with Fe(III) heme–thiolate proteins.[13] However, under conditions of even a small excess of NO, the initially formed NO complex of **4** proved to be very unstable; i.e., subsequent attack of a second NO on the sulfur atom of the RS$^-$ group was clearly observed.[13]

It was anticipated that these problems would not be encountered when employing complex **2**, since the RSO$_3^-$ group replacing the thiolate ligand (i) is less accessible due to steric hindrance and (ii) is "forced" into coordination to iron because the ligand belongs to a bridge spanning the porphyrin. The present work was undertaken to evaluate thermodynamic and kinetic data for NO binding to iron(III) of the high-spin complex **2** ($g = 5.67, 2.03$), which is insoluble in water but soluble in organic solvents such as CH$_2$Cl$_2$, CHCl$_3$, BuCN, toluene, and methanol. To investigate the influence of the iron(III) coordination sphere on the dynamics of the reaction with NO, the studies were carried out in non-coordinating toluene and in coordinating methanol. In toluene the five-coordinate complex **2**, reminiscent of the E·S complex of P450$_{cam}$, is produced, whereas in methanol the six-coordinate complex **5** should be formed, resembling the resting state of P450$_{cam}$. Employing low-temperature stopped-flow and laser flash photolysis techniques at ambient and high pressure, suitable rate and activation parameters can be derived that reveal insight into the mechanisms for the "on" and "off" processes for NO binding and allow a comparison of the model systems with the corresponding states of cytochrome P450.

Experimental Section

Materials. All solutions were prepared in toluene (puriss from Aldrich or Acros Organics) or methanol (≥99.9% from Roth). Complex **2** was prepared as described in the literature and characterized by UV–vis, EPR, and ESI-MS spectroscopy.[8] All other chemicals used throughout this study were of analytical reagent grade. NO gas, purchased from Riessner Gase or Linde 93 in a purity of at least 99.5 vol %, was cleaned to remove trace amounts of higher nitrogen oxides such as N$_2$O$_3$ and NO$_2$ by passing it through an Ascarite II column (NaOH on silica gel, Sigma-Aldrich) and then bubbling through a gas scrubbing bottle containing 5 M NaOH (Aldrich).

Solution Preparation. All solutions were prepared under strict exclusion of air. Toluene was distilled from a purple solution of benzophenone over sodium under Ar directly before use. Methanol was deaerated for extended periods with pure Ar before it was brought in contact with complex **2** or NO. The concentration of NO in NO-saturated methanol was determined with the NO electrode to be 0.014 M at 23 °C. The concentration of NO at saturation in toluene was

assumed to be 0.011 M at 25 °C.[14] Dilutions of known concentration were prepared from these saturated solutions by a syringe technique.

NO Electrode Measurements. The concentration of free NO in methanol was determined with an ISO-NOP electrode connected to an ISO-NO Mark II NO sensor from World Precision Instruments.[15] To determine the concentration of NO in methanol solutions, the following procedure was followed. A known volume of the NO-saturated methanol solution (at 23 °C) was dropped into a known volume of degassed water. The concentration of NO in the resulting solution was measured with the NO electrode. The NO electrode was calibrated daily with fresh solutions of sodium nitrite and potassium iodide according to the method suggested by the manufacturer. The calibration factor nA/μM was determined with a linear fit program.

UV–Vis Measurements. UV–vis spectra at appropriate temperatures were recorded in gastight cuvettes on a Shimadzu UV-2100 spectrophotometer equipped with a thermostated cell compartment CPS-260. A pill-box cell combined with high-pressure equipment[16] was used to record UV–vis spectra under high pressure (up to 150 MPa).

EPR Measurements. To investigate the spin state of **2** in the presence of an excess of nitric oxide (nitrosyl complex of **2**) and methanol (complex **5**), cw-EPR experiments were carried out using a Bruker ESP-300 X-band spectrometer equipped with a T$_{102}$ cell and an ER 4111 VT liquid nitrogen cryostat. EPR measurements of the nitrosyl complex of **2** were performed under strict exclusion of air oxygen.

FTIR Measurements. FTIR measurements on complex **2** in the presence of a large excess of NO were performed in toluene under exclusion of air oxygen at ~5 °C. The spectra were recorded with Mattson Infinity FT/IR-60 AR spectrophotometer.

Laser Flash Photolysis. Laser flash photolysis kinetic studies were carried out with an LKS.60 spectrometer from Applied Photophysics for detection and a Nd:YAG laser (SURLITE I-10 Continuum) pump source operating in the second harmonics ($\lambda_{exc} = 532$ nm, 245 mJ pulses with ~7 ns pulse widths). Spectral changes at appropriate wavelength were monitored using a 100 W xenon arc lamp, monochromator, and PMT-1P22 photomultiplier tube. The absorbance reading was balanced to zero before the flash, and data were recorded on a DSO HP 54522A digital storage oscilloscope and then transferred to a personal computer for subsequent analysis. Gastight quartz cuvettes and a pill-box cell combined with high-pressure equipment[16] were used at ambient and high pressure (up to 150 MPa), respectively. At least 10 kinetic runs were recorded under all conditions, and the reported rate constants represent the mean value of these.

Low-Temperature Stopped-Flow Instrument and Software. Time-resolved UV–vis spectra were recorded with a Hi-Tech SF-3L low-temperature stopped-flow unit (Hi-Tech Scientific, Salisbury, UK) equipped with a J&M TIDAS 16/300-1100 diode array spectrophotometer (J&M, Aalen, Germany). The optical cell had a light path of 1.0 cm and was connected to the spectrophotometer unit with flexible light guides. Five-milliliter driving syringes were used. The mixing chamber was immersed in an ethanol bath which was placed in a Dewar flask containing liquid nitrogen. The ethanol bath was cooled by liquid nitrogen evaporation, and its temperature was measured by use of a Pt resistance thermometer and maintained to ±0.1 °C by using a PID temperature-controlled thyristor heating unit (both Hi-Tech). Complete spectra were collected between 400 and 760 nm with the integrated J&M software Kinspec 2.30.

All kinetic experiments were performed under pseudo-first-order conditions, i.e., at least a 10-fold excess of NO. The studied reactions exhibited pseudo-first-order behavior for at least three half-lives. In all stopped-flow experiments, at least five kinetic runs were recorded

(11) (a) Walker, F. A. *J. Inorg. Biochem.* **2005**, *99*, 216. (b) Ding, X. D.; Weichsel, A.; Andersen, J. F.; Shokhireva, T. Th.; Balfour, C.; Pierik, A. J.; Averill, B. A.; Mantfort, W. R.; Walker, F. A. *J. Am. Chem. Soc.* **1999**, *121*, 128. (c) Weichsel, A.; Maes, E. M.; Andersen, J. F.; Valenzuela, J. G.; Shokhireva, T. Kh.; Walker, F. A.; Montfort, W. R. *Proc. Natl. Acad. Sci. U.S.A.* **2005**, *102*, 594.

(12) Franke, A.; Stochel, G.; Jung, C.; van Eldik, R. *J. Am. Chem. Soc.* **2004**, *126*, 4181.

(13) Franke, A.; Stochel, G.; Suzuki, N.; Higuchi, T.; Okuzono, K.; van Eldik, R. *J. Am. Chem. Soc.* **2005**, *127*, 5360.

(14) Shaw, A. W.; Vosper, A. J. *J. Chem. Soc., Faraday Trans. 1* **1977**, *73*, 1239.

(15) Kudo, S.; Bourassa, J. S. E.; Sato, Y.; Ford, P. C. *Anal. Biochem.* **1997**, *247*, 193.

(16) Spitzer, M.; Gartig, F.; van Eldik, R. *Rev. Sci. Instrum.* **1988**, *59*, 2092.
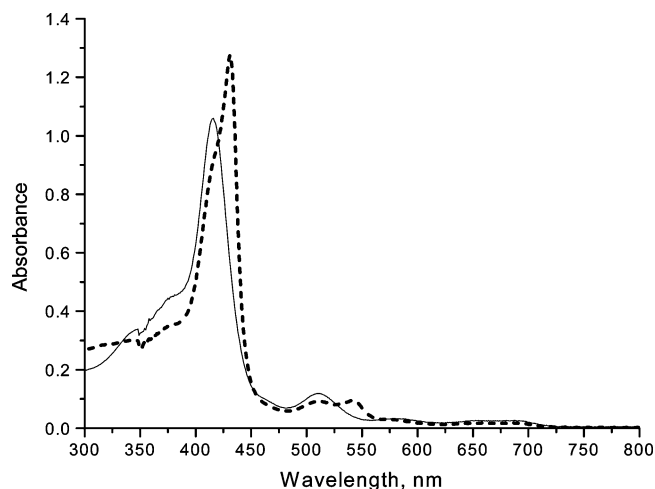
Figure 2. Electronic absorption spectra of **2** before (solid line) and after saturation with NO (dashed line) in toluene solution. Experimental conditions: [**2**] = 4.5×10^{-6} M, [NO] = 1.1×10^{-2} M, 20 °C.

under all conditions, and the reported rate constants represent the mean values. The activation parameters and corresponding error limits were calculated from a weighted linear least-squares fit of the data.

Results

I. Reaction of Complex 2 with Nitric Oxide in Toluene. A. Effect of Temperature and Pressure on the Equilibrium Constant, K_{NO}. The UV–vis spectrum of **2** in toluene solution exhibits a Soret band maximum at 416 nm and a Q-band at 512 nm (Figure 2). Exposure of a degassed solution of **2** to *a large excess* of NO gas leads to spectral shifts of the Soret and Q-bands to 432 and 542 nm, respectively. The uptake of NO appears to be completely reversible, as judged from experiments in which a stream of Ar gas was used to remove NO from solution, consistent with the equilibrium described by eq 1. It

$$2 + NO \underset{k_{off}}{\overset{k_{on}}{\rightleftharpoons}} 2(NO) \qquad K_{NO} \qquad (1)$$

should be noted that the same reaction carried out with a NO-saturated toluene solution ([NO] = 0.0055 M after mixing) at 20 °C resulted in the formation of only a very small fraction of the nitrosyl complex (only a weak shoulder at 432 nm). This result suggests that the equilibrium of the nitrosylation reaction (eq 1) is *strongly* shifted to the left side at room temperature. The effect of temperature on the equilibrium described by eq 1 was studied over the temperature range from 5 to 38 °C (Figure 3a). The values of the equilibrium constants for eq 1 (K_{NO}^{tol}), calculated from the spectral changes over the temperature range 15–38 °C, are summarized in Table 1.

The temperature dependence of $\ln(K_{NO}^{tol})$ (Figure 3a, inset) was found to be linear and gave significantly negative values for the thermodynamic parameters $\Delta H°$ and $\Delta S°$ (Table 1). The effect of pressure on the equilibrium constant K_{NO}^{tol} was examined in the pressure range 5–150 MPa (Figure 3b). The pressure dependence of $\ln(K_{NO}^{tol})$ gave a straight line (Figure 3b, inset) and resulted in $\Delta V°_{NO} = -39 \pm 2$ cm^3 mol^{-1}.

B. FTIR and EPR Characterization of the Nitrosyl Product, 2(NO). FTIR measurements on a toluene solution of **2** under a large excess of NO revealed formation of a new species (Figure 4a). The difference FTIR spectrum of **2**(NO) and **2** (Figure 4b) shows a sharp band at 1833 cm^{-1}, which is
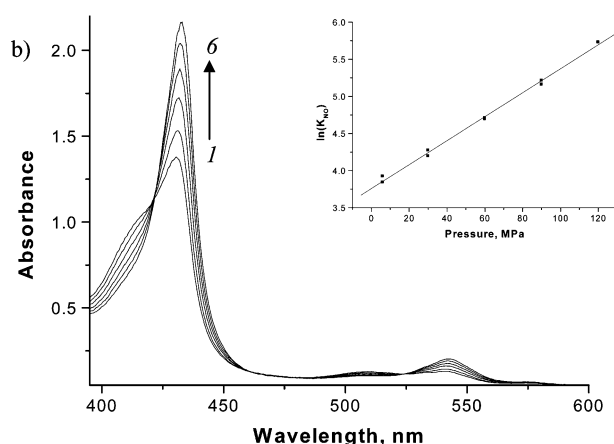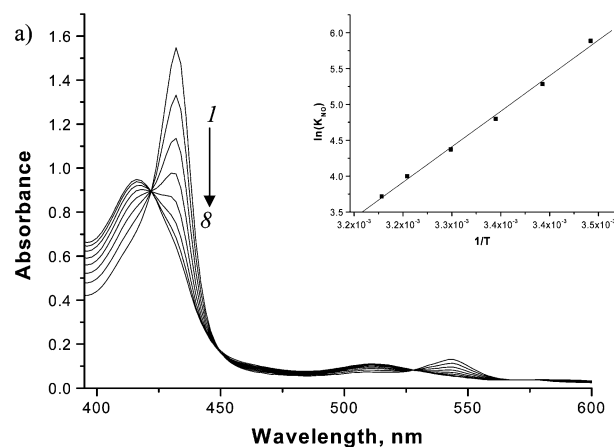
Figure 3. Spectral changes recorded for the reaction between **2** and NO in toluene. (a) As a function of temperature, from 5 (line 1) to 38 °C (line 8); inset, temperature dependence of $\ln(K_{NO})$. Experimental conditions: [**2**] = 4×10^{-6} M, [NO] = 0.0045 M. (b) As a function of pressure, from 5 (line 1) to 150 MPa (line 6); inset, $\ln(K_{NO})$ as a function of pressure. Experimental conditions: [**2**] = 4.5×10^{-6} M, [NO] = 0.011 M, 25 °C.

Table 1. Temperature and Pressure Dependence of K_{NO}^{tol} for the Reaction of **2** with NO in Toluene

T (°C)	P (MPa)	K_{NO} (M^{-1})
15	0.1	360 ± 17
20		197 ± 14
25		122 ± 10
30		79 ± 9
35		54 ± 6
38		41 ± 4
25	5	123 ± 9
	30	175 ± 11
	60	270 ± 13
	90	450 ± 16
	120	752 ± 15
$\Delta H°_{NO}$ (kJ mol^{-1})		-71 ± 3
$\Delta S°_{NO}$ (J mol^{-1} K^{-1})		-197 ± 10
$\Delta G°_{NO}$ (kJ mol^{-1}) at 25 °C		-12 ± 3
$\Delta V°_{NO}$ (cm^3 mol^{-1})		-39 ± 2

very close to the N–O stretching modes found for nitrosyl complexes of natural heme–thiolate-containing enzymes such as P450$_{nor}$[17a] and P450$_{cam}$[17a,b] (ν_{N-O} = 1853 and 1806 cm^{-1}, respectively) and synthetic heme–thiolate-ligated models such
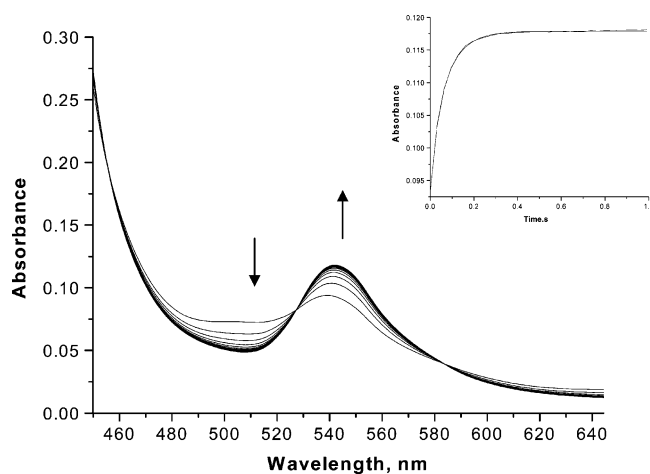
(17) (a) Obayashi, E.; Tsukamoto, K.; Adachi, S.; Takahashi, S.; Nomura, M.; Iizuka, T.; Shoun, H.; Shiro, Y. *J. Am. Chem. Soc.* **1997**, *119*, 7807. (b) Hu, S.; Kincaid, J. R. *J. Am. Chem. Soc.* **1991**, *113*, 2843.
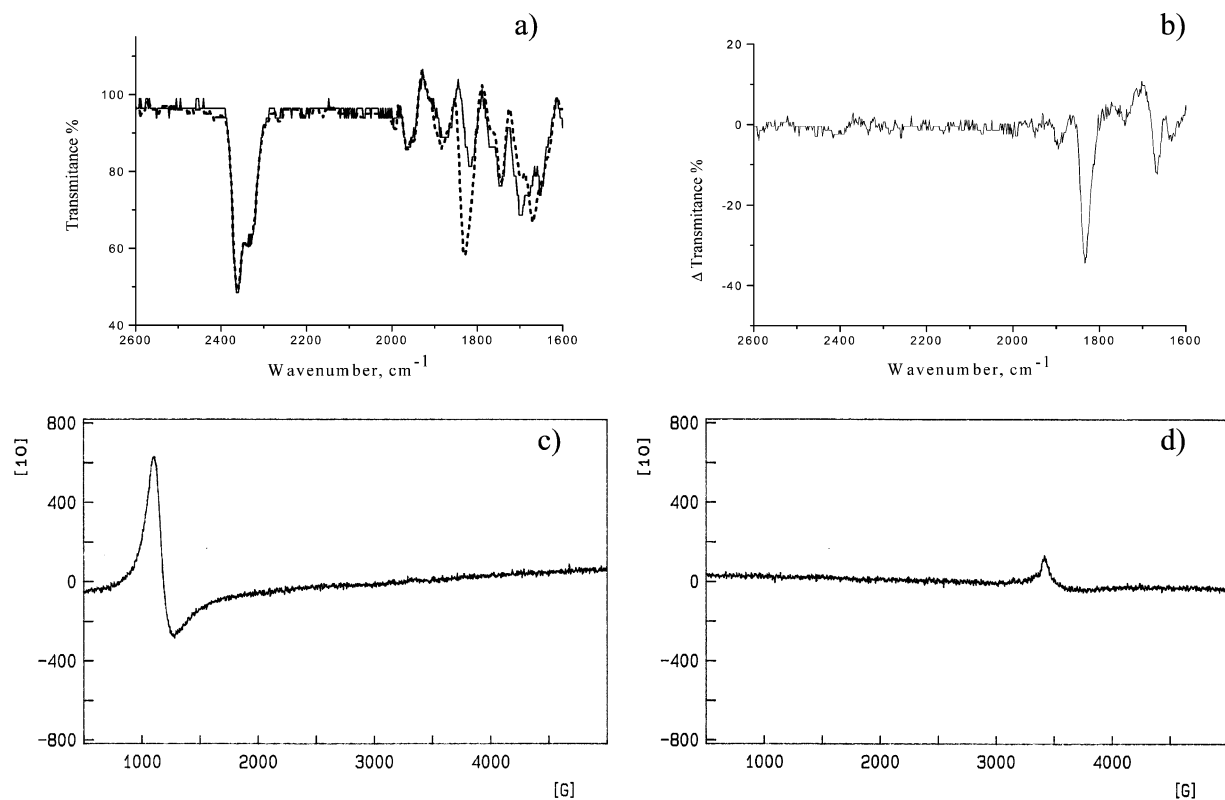
Figure 4. (a) FTIR spectra of a toluene solution of complex **2** before (solid line) and after saturation with NO gas (dashed line), measured at 5 °C. (b) The difference FTIR spectrum of toluene solutions of **2** and **2**(NO). (c,d) EPR spectra of a toluene solution of **2** before and after saturation with NO gas, respectively.

as SR[4a] and SR-HB[4h] (ν_{N-O} = 1828 and 1837 cm^{-1}, respectively[18]). To investigate the Fe(III) spin state of the complex **2**(NO), the EPR spectrum of a degassed toluene solution of **2** was recorded before and after NO saturation (Figure 4c,d). The spectrum of the nitrosyl complex shows a complete disappearance of the signal at g = 5.78 (characteristic for the high-spin complex **2**) and appearance of a weaker new signal at g = 1.98. The nitrosylation reaction appears to be completely reversible as judged from the EPR spectrum recorded after the removal of NO from the solution by bubbling through a stream of Ar (the spectrum displays complete recovery of the signal at g = 5.78; spectrum not shown). To investigate the nature of the signal at g = 1.98, obtained by treatment of a toluene solution of **2** with an excess of NO, an experiment was performed wherein degassed toluene was saturated with NO and an EPR spectrum was recorded for the so-prepared solution (Figure S1, Supporting Information). As judged from this spectrum and a comparison with the spectrum obtained in the EPR experiments for the **2**(NO) complex (Figure 4d), it is persuasive to interpret the signal at g = 1.98 in the latter as stemming from an excess of NO in the complex solution.

C. Low-Temperature Stopped-Flow Study of the "On" Reaction. At room temperature, the "on" reaction described by eq 1 was found to be too fast for stopped-flow studies. However, the use of a low-temperature stopped-flow instrument enabled us to measure the rate of this reaction in the NO concentration range $(1.4-4.1) \times 10^{-5}$ M over the temperature range from −70 to −40 °C. Typical spectral changes for nitric oxide binding to complex **2** (Q band), recorded with the rapid-scan, low-

(18) Suzuki, N.; Higuchi, T.; Urano, Y.; Kikuchi, K.; Uchida, T.; Mukai, M.; Kitagawa, T.; Nagano, T. *J. Am. Chem. Soc.* **2000**, *122*, 12059.

Figure 5. Spectral changes of the Q-band region recorded during NO binding to **2** in toluene at −70 °C. Experimental conditions: **[2]** = 1.5 × 10^{-6} M, [NO] = 1.4 × 10^{-5} M, spectra recorded within 0−1 s after mixing. Inset: Typical absorbance−time plot for NO binding to **2**, recorded at 542 nm under these conditions.

temperature stopped-flow instrument, are shown in Figure 5. A typical kinetic trace, recorded at 542 nm at −70 °C for NO binding to **2** in toluene, is shown in the inset of Figure 5.

The rate of reaction (1) with NO in excess is expected to follow pseudo-first-order kinetics, for which the observed rate constant, k_{obs}, can be expressed by eq 2. Plots of k_{obs} versus

$$k_{obs} = k_{on}[NO] + k_{off} \qquad (2)$$

[NO] were linear at all temperatures (Figure S2, Supporting Information), and the resulting k_{on} values are summarized in

Table 2. k_{on} and k_{off} Values and Activation Parameters for the Reversible Binding of NO to Complex **2** in Toluene As Measured with the Low-Temperature Stopped-Flow Technique

T (°C)	$k_{on} \times 10^{-6}$ (M^{-1} s^{-1})	k_{off} (s^{-1})
−70	0.79 ± 0.09	−3 ± 3
−60	0.89 ± 0.06	1 ± 2
−50	0.99 ± 0.09	5 ± 3
−45	1.04 ± 0.03	9.2 ± 0.8
−40	1.08 ± 0.05	14 ± 1
$\Delta H^{\ddagger}$ (kJ mol^{-1})	2.3 ± 1.0	43 ± 10
$\Delta S^{\ddagger}$ (J mol^{-1} K^{-1})	−118 ± 5	−38 ± 42
$\Delta G^{\ddagger}$ (kJ mol^{-1}) at 25 °C	37 ± 1	54 ± 10

Table 2. They appeared not to be very temperature sensitive (the relatively large change in temperature from −70 to −40 °C resulted in only a small change in the k_{on} values). A linear Eyring plot of these data gave a very small value for the activation enthalpy and a significantly large and negative value for the activation entropy (Table 2).

D. Kinetics of the Dissociation of NO from the 2(NO) Complex. The reaction described by eq 1 appears to be completely reversible. At room temperature, the equilibrium is strongly shifted to the left side. In principle, k_{off} could be directly determined from the experiment in which the **2**/**2**(NO) equilibrium is disturbed via dilution. Indeed, mixing of the **2**/**2**(NO) equilibrium solution with deoxygenated toluene resulted in the rapid formation of complex **2**. However, attempts to determine k_{off} in the temperature range 5−20 °C using the stopped-flow technique failed. The back reaction (binding of NO) appeared to be too fast between 5 and 20 °C, and only the end of this reaction could be observed using the stopped-flow technique. At lower temperatures (<5 °C), the **2**(NO) complex is more stable and dilution did not have an effect on the reaction; i.e., only formation of the nitrosylation product is seen after dilution with toluene.

In principle, the NO dissociation rate constant at lower temperatures can be obtained from the intercept of the plot of k_{obs} vs [NO] at the appropriate temperature (see Table 2). However, it should be noted that these values are subject to a relatively large extrapolation error, and the small values of k_{off} cannot be determined accurately in this manner (for example, k_{off} values at −70 or −60 °C are close to zero). The linear Eyring plot of $\ln(k_{off}/T)$ vs $1/T$ resulted in a relatively high activation enthalpy and a small value for the activation entropy.

The values of the reaction parameters ($\Delta H° = \Delta H^{\ddagger}_{on} - \Delta H^{\ddagger}_{off}$ and $\Delta S° = \Delta S^{\ddagger}_{on} - \Delta S^{\ddagger}_{off}$) calculated on the basis of the kinetic data in Table 2 agree rather poorly with those obtained from the thermodynamic experiments. However, this apparent discrepancy can be easily explained in terms of the relatively large extrapolation errors in the determination of the values of the activation parameter for the forward and back reactions. Therefore, it seems more reasonable to calculate the free energy $\Delta G°$ for the overall reaction (1) from the kinetic ΔG values, which should give a more reliable value due to partial compensation effects that occur in the activation parameters ΔH and ΔS. Indeed, the value of $\Delta G°$ obtained from the kinetic data at 298 K ($\Delta G°_{298} = -17 \pm 11$ kJ mol^{-1}) is, within experimental error, very close to that obtained in the thermodynamic studies ($\Delta G°_{298} = -12 \pm 3$ kJ mol^{-1}).

E. Laser Flash Photolysis Kinetics. Laser flash photolysis can be employed to study the kinetics of a reaction on a
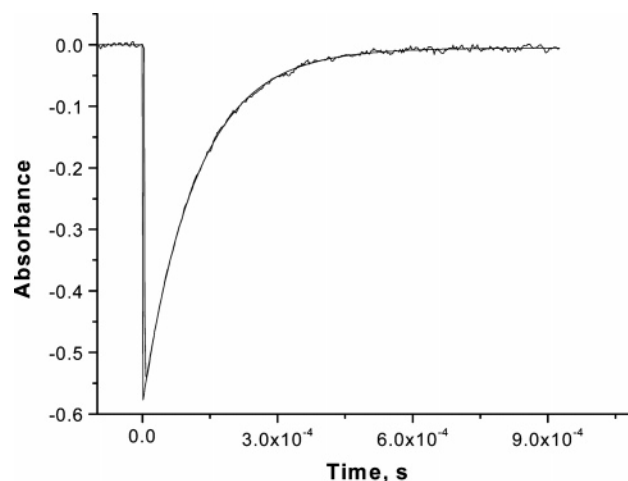
Figure 6. Typical flash photolysis kinetic trace recorded at 435 nm for the formation of the **2**(NO) complex. Experimental conditions: [**2**] = 1 × 10^{-5} M, [NO] = 0.0037 M in toluene at 5 °C, λ_{exc} = 532 nm.

Scheme 1
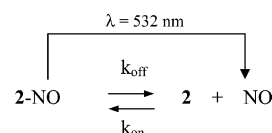
significantly faster time scale than the stopped-flow method. Therefore, this technique enabled us to measure the rate constants for NO binding to complex **2** (k_{obs}) in a much higher NO concentration range (mM) and in a more accurate way (k_{obs} values obtained from the rapid-scan stopped-flow method are subject to larger fitting errors due to the limited number of points present for each kinetic trace). Laser flash irradiation at 532 nm of an equilibrium mixture of complex **2** and **2**(NO) leads to labilization of NO from the latter complex and relaxation of the non-steady-state system back to the original equilibrium position, which can be followed spectrophotometrically according to Scheme 1. The decay of the transient was followed using single-wavelength detection at 435 nm and fitted to a single-exponential function. A typical flash photolysis kinetic trace recorded for NO binding to complex **2** is shown in Figure 6.

The observed rate constant, k_{obs}, increases linearly with increasing NO concentration in the temperature range 5−30 °C, with very large values for the intercepts (see Figure S3, Supporting Information). The values of k_{on} and k_{off} obtained from the slopes and intercepts of these plots, respectively, are summarized in Table 3. The temperature dependence of k_{on} and k_{off} was used to construct Eyring plots for the forward and back reactions. The activation parameters for NO binding are characterized by a very small value of $\Delta H^{\ddagger}_{on}$ and a large and negative value for $\Delta S^{\ddagger}_{on}$ (Table 3). They are in good agreement with the activation parameters ($\Delta H^{\ddagger}_{on}$ and $\Delta S^{\ddagger}_{on}$) obtained above from the low-temperature stopped-flow experiments (see Table 2). The activation enthalpy and entropy for NO dissociation from **2**(NO) were found to be more positive and more accurate than those determined by low-temperature stopped-flow measurements (see experimental error limits on $\Delta H^{\ddagger}_{off}$ and $\Delta S^{\ddagger}_{off}$ in Tables 2 and 3). Accordingly, the value of $\Delta G°$ for reaction (1) obtained from the flash-photolysis studies ($\Delta G° = -13 \pm 4$ kJ mol^{-1} at 298 K) is very close to the value of the free energy determined in the thermodynamic studies.
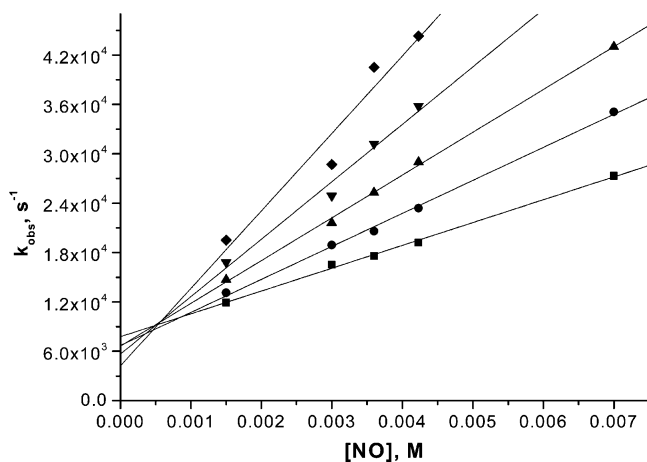
Figure 7. Plots of k_{obs} vs [NO] for the reaction of **2** with NO over the pressure range of 30–150 MPa as measured by laser flash photolysis at 30 (■), 60 (●), 90 (▲), 120 (▼), and 150 MPa (◆). Experimental conditions: [**2**] = 5 × 10^{-6} M, [NO] = 0.0015–0.007 M in toluene at 20 °C, λ_{exc} = 532 nm, λ_{det} = 435 nm.

Table 3. Rate Constants and Activation Parameters for NO Binding to Complex **2** As Determined by Laser Flash Photolysis

T (°C)	P (MPa)	$k_{on} \times 10^{-6}$ (M^{-1} s^{-1})	k_{off} (s^{-1})
5	0.1	1.5 ± 0.1	2350 ± 300
10		1.5 ± 0.2	3770 ± 550
15		1.6 ± 0.1	5570 ± 360
20		1.7 ± 0.1	8470 ± 240
25		1.80 ± 0.05	12470 ± 120
30		1.88 ± 0.07	18630 ± 180
20	30	2.77 ± 0.08	7770 ± 330
	60	4.0 ± 0.1	6710 ± 490
	90	5.2 ± 0.1	6620 ± 480
	120	7.0 ± 0.7	5660 ± 2230
	150	9 ± 2	4220 ± 5230
ΔH (kJ mol^{-1})		4 ± 2	58 ± 2
ΔS (J mol^{-1} K^{-1})		−111 ± 6	+29 ± 5
ΔG (kJ mol^{-1}) at 25 °C		37 ± 2	50 ± 2
ΔV (cm^3 mol^{-1})		−25 ± 1	+7 ± 3

The effect of pressure on NO binding to complex **2** in toluene was studied at 20 °C over a NO concentration range from 0.0015 to 0.007 M. From plots of k_{obs} vs [NO] at different pressures (P) (Figure 7), values of k_{on} and k_{off} were determined and are summarized in Table 3. The linear plots of ln(k_{on}) vs P and ln(k_{off}) vs P (Figure S4, Supporting Information) clearly show that the NO binding rate constant (k_{on}) increases significantly with increasing pressure, whereas the NO dissociation rate constant (k_{off}) decreases with increasing pressure. The resulting value of the activation volume was found to be large and negative for the "on" reaction and much smaller (in absolute value) and positive for the dissociation reaction. The reaction volume $\Delta V°$ for the overall equilibrium ($\Delta V° = \Delta V^{\ddagger}_{on} - \Delta V^{\ddagger}_{off}$) is substantially large and negative, viz. −32 ± 4 cm^3 mol^{-1} which is in good agreement with the value of $\Delta V°$ found in our thermodynamic studies, viz. −39 ± 2 cm^3 mol^{-1}. Thus, there is a significant overall change in the partial molar volume during NO binding to complex **2**.

II. Reaction of Complex 2 with Nitric Oxide in Methanol. A. Coordination Environment and Spin State of 2(Fe^{III}) in Methanol. The electronic absorption spectrum of **2** in methanol exhibits two bands in the Soret region (396 and 416 nm) and a Q-band at 532 nm. Titration of the toluene solution of **2** with

methanol leads to the partial disappearance of the bands at 416 and 512 nm (characteristic of the five-coordinate complex **2**) with concomitant formation of new bands at 396 and 532 nm (Figure S5, Supporting Information). The spectra display clean isosbestic points, indicating that the equilibrium is simply expressed as shown in eq 3.

$$2 + \text{MeOH} \underset{}{\overset{K_{MeOH}}{\rightleftharpoons}} 5 \qquad (3)$$
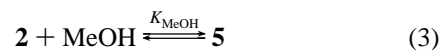
The equilibrium constant, K_{MeOH}, determined from the spectral changes appeared to be rather small and equals 0.20 ± 0.05 M^{-1} at 25 °C. The effect of temperature and pressure on equilibrium (3) was studied over the temperature range 4–40 °C and the pressure range 0.1–150 MPa. The values of K_{MeOH} were calculated from the spectral changes in the same way as for the reaction of **2** with NO. The linear plots of ln(K_{MeOH}) vs $1/T$ or P (Figure S6, Supporting Information) gave the reaction parameters: $\Delta H°_{MeOH}$ = −13.9 ± 0.2 kJ mol^{-1}, $\Delta S°_{MeOH}$ = −33.7 ± 0.8 J mol^{-1} K^{-1}, and $\Delta V°_{MeOH}$ = −6.5 ± 0.2 cm^3 mol^{-1}.

To investigate the spin state of **2** in the presence of methanol, 0.57 mg of complex **2** was dissolved in degassed toluene (0.1 mL), and EPR spectra were measured upon subsequent addition of MeOH. For a MeOH/toluene ratio of up to 2/1, no low-spin signals could be detected (Figure S7a, Supporting Information), the only obvious changes in the spectrum being a slight broadening and shift of the signal at g = 5.8 to 5.6 and a decrease of the signal intensity due to dilution of the sample. The same result (high-spin signal) was obtained when complex **2** (0.52 mg) was dissolved in degassed MeOH (0.1 mL) and EPR spectra were measured upon subsequent addition of toluene. Although the matrix prevented an adequate analysis for pure MeOH solution, the recorded spectrum still adumbrates a high-spin iron(III) species. Another scenario was observed when complex **2** (0.56 mg) was dissolved in degassed toluene (0.1 mL) but was then treated with a saturated MeOK/MeOH solution, instead of methanol. The spectrum after addition of 50 μL of MeOK/MeOH displays dominant signals of the low-spin iron(III) complex, g = 2.42, 2.15, and 1.93 (Figure S7b, Supporting Information).

B. Thermodynamics of NO Binding to Complex 5. Exposure of the degassed methanol solution of **5** to an excess of NO gas leads to the formation of a new species characterized by Soret and Q-bands at 424 and 542 nm, respectively (Figure 8). The binding of NO to **5** in methanol was shown to be completely reversible, consistent with the equilibrium expressed in eq 4.

$$5 + \text{NO} \underset{}{\overset{K_{NO}^{met}}{\rightleftharpoons}} 2(\text{NO}) + \text{MeOH} \qquad (4)$$
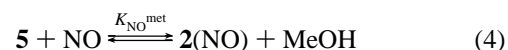
However, the reaction carried out with NO-saturated methanol solution ([NO] = 0.007 M after mixing) at 20 °C resulted in the formation of only a very small fraction of the nitrosyl complex. The behavior observed was the same as for the reaction carried out in toluene solution and indicates that the equilibrium in reaction (4) is also strongly shifted to the left at room temperature.

As for the binding of NO to **2** in toluene, equilibrium (4) is also strongly affected by temperature and pressure (Figure S8a,b, Supporting Information). The values of the equilibrium constants K_{NO}^{met}, calculated from the spectral changes at various tem-
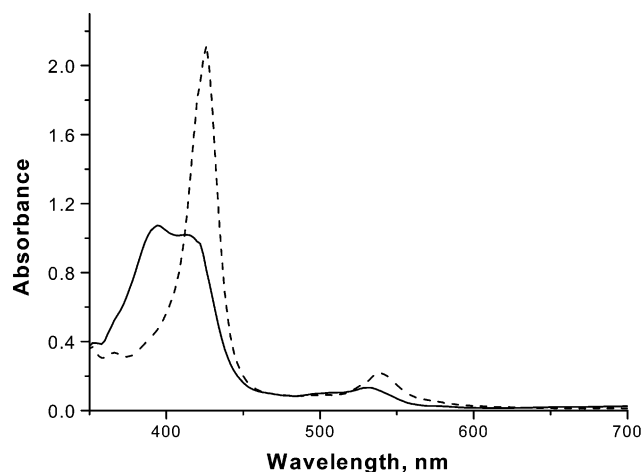
Figure 8. Electronic absorption spectra of **5** before (solid line) and after saturation with NO (dashed line) in methanol solution. Experimental conditions: $[5] = 1.2 \times 10^{-5}$ M, $[NO] = 1.41 \times 10^{-2}$ M, ~ 0 °C.

Table 4. Values of K_{NO}^{met} and Thermodynamic Parameters for the Binding of NO to **5** in Methanol

T (°C)	P (MPa)	K_{NO}^{met} (M^{-1})
5	0.1	142 ± 10
10		92 ± 6
15		61 ± 4
20		38 ± 4
25		26 ± 3
25	0.1	27 ± 2
	50	59 ± 2
	100	111 ± 6
	150	162 ± 9
$\Delta H^{\circ}{}_{NO}^{met}$ (kJ mol^{-1})		-59 ± 4
$\Delta S^{\circ}{}_{NO}^{met}$ (J mol^{-1} K^{-1})		-169 ± 13
$\Delta G^{\circ}{}_{NO}^{met}$ (kJ mol^{-1}) at 25 °C		-9 ± 4
$\Delta V^{\circ}{}_{NO}^{met}$ (cm^3 mol^{-1})		-28 ± 1

peratures and pressures, are summarized in Table 4. The temperature and pressure dependence of K_{NO}^{met} gave good straight-line fits (insets of Figure S8a,b) and resulted in significantly large and negative thermodynamic parameters (Table 4).

C. Low-Temperature Stopped-Flow Study on the Reversible Binding of NO to Complex 5 in Methanol. The binding of NO to **5** was studied in methanol in the NO concentration range from 7.6×10^{-4} to 3.8×10^{-3} M over the temperature range from -80 to -40 °C with the use of the rapid-scan, low-temperature stopped-flow instrument. Typical spectral changes and a kinetic trace recorded for this reaction in methanol at 424 nm are shown in Figure S9 (Supporting Information). k_{obs} values increase linearly with increasing [NO] for all the studied temperatures (Figure S10, Supporting Information). The values of the binding and dissociation rate constants obtained from the slopes and intercepts of these plots, respectively, are summarized in Table 5.

The linear Eyring plot of the data in Table 5 resulted in a relatively small value for the activation enthalpy and a negative value for the activation entropy (but more positive than found for these parameters in toluene). The activation parameters (especially activation entropy) for the back reaction were determined less accurately due to large extrapolation errors in determining the k_{off} values. However, the value of the free energy calculated from these data ($\Delta G^{\circ} = -8 \pm 6$ kJ mol^{-1} at

Table 5. Rate and Activation Parameters for NO Binding to **5** in Methanol

T (°C)	$k_{on} \times 10^{-3}$ (M^{-1} s^{-1})	k_{off} (s^{-1})
-80	1.4 ± 0.1	0.06 ± 0.25
-70	2.5 ± 0.2	0.31 ± 0.50
-60	4.1 ± 0.1	1.31 ± 0.24
-50	5.8 ± 0.1	3.9 ± 0.2
-40	8.5 ± 0.8	12 ± 2
$\Delta H^{\ddagger}$ (kJ mol^{-1})	14 ± 0.7	44 ± 5
$\Delta S^{\ddagger}$ (J mol^{-1} K^{-1})	-107 ± 3	-34 ± 22
$\Delta G^{\ddagger}$ (kJ mol^{-1}) at 25 °C	46 ± 1	54 ± 5

298 K) is in close agreement with that determined in the thermodynamic studies.

D. Stability of the 2(NO) Complex in Methanol. **2**(NO) appeared not to be stable in methanol. Over a longer time under an excess of NO, the nitrosyl complex of **2** undergoes a subsequent slow reaction characterized by a shift in the Soret band to 413 nm, with a concomitant increase in absorbance (Figure S11, Supporting Information). These slow absorbance changes following **2**(NO) complex formation were not observed in toluene under the same conditions. However, it should be noted that a similar slow reaction was also observed for NO binding to **4** in methanol.[13] Based on reports in the literature, methanol can induce a nucleophilic attack at coordinated nitrosyl (NO$^+$) and lead to reductive nitrosylation of ferric porphyrins.[19] In addition, nitrite impurities can also catalyze the reductive nitrosylation of ferri-heme systems.[20] We therefore suggest that the second slow reaction leads to the formation of $2(Fe^{II})(NO)$ as a final product. This suggestion was confirmed by an experiment in which first complex **5** was reduced to $2(Fe^{II})$ with NaBH$_4$ in methanol (Figure S12, Supporting Information, line 2) and then the reduced complex was treated with NO (line 3). The spectrum of $2(Fe^{II})(NO)$ is characterized by a band at 413 nm and seems to be indistinguishable from the spectrum of the final product obtained when complex **5** was treated with an excess of NO over a longer time.

Discussion

Suggested Mechanism for the Formation of 2(NO) in Toluene. The thermal activation parameters for the "on" reaction described by eq 1 show a very small value for $\Delta H^{\ddagger}_{on}$ and a substantially negative value for $\Delta S^{\ddagger}_{on}$. These features are consistent with the mechanism proposed earlier for NO binding to iron(II) heme proteins[21] and other heme model systems.[22] The same mechanism was also suggested for NO binding to cytochrome P450$_{cam}$ in the presence of the substrate (camphor).[12] In such a mechanism, an encounter complex is formed prior to Fe−NO bond formation, according to eq 5, where k_D is the rate constant for the diffusion-controlled formation of the encounter complex, k_{-D} is the rate constant for the dissociation of the

(19) (a) Mu, X. H.; Kadish, K. M. *Inorg. Chem.* **1988**, *27*, 4720. (b) Gwost, D.; Caulton, K. G. *J. Chem. Soc., Chem. Commun.* **1973**, 64. (c) Gwost D.; Caulton, K. G. *Inorg. Chem.* **1973**, *12*, 2095.
(20) (a) Fernandez, B. O.; Ford, P. C. *J. Am. Chem. Soc.* **2003**, *125*, 10510. (b) Fernandez, B. O.; Lorkovi, I. M.; Ford, P. C. *Inorg. Chem.* **2003**, *42*, 2. (c) Fernandez, B. O.; Lorkovi, I. M.; Ford, P. C. *Inorg. Chem.* **2004**, *43*, 5393.
(21) (a) Taube, D. J.; Projahn, H. D.; van Eldik, R.; Magde, D.; Traylor, T. G. *J. Am. Chem. Soc.* **1990**, *112*, 6880. (b) Tetreau, C.; Di Primo, C.; Lange, R.; Tourbez, H.; Lavalette, D. *Biochemistry* **1997**, *36*, 10262. (c) Ansari, A.; Jones, C. M.; Henry, E. R.; Hofrichter, J.; Eaton, W. A. *Biochemistry* **1994**, *33*, 5128.
(22) Laverman, L. E.; Ford, P. C. *J. Am. Chem. Soc.* **2001**, *123*, 11614.

$$2 + NO \underset{k_{-D}}{\overset{k_D}{\rightleftharpoons}} \{2||NO\} \underset{k_{-a}}{\overset{k_a}{\rightleftharpoons}} 2(NO) \quad (5)$$
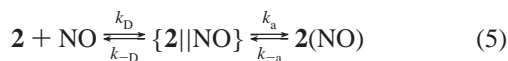
encounter complex, and k_a is that for the "activation" step in which the Fe—NO bond is formed. On the basis of the steady-state approximation for the encounter complex, the observed rate constant can be expressed by eq 6, where $k_{on} = k_a k_D/(k_a +$

$$k_{obs} = \frac{k_a k_D}{k_a + k_{-D}}[NO] + k_{-a} \quad (6)$$

$k_{-D})$ and $k_{off} = k_{-a}$. The value of the second-order rate constant, k_{on}, for the binding of NO to **2** was found to be many orders of magnitude smaller than that for diffusion-controlled reactions in toluene (viz., the rate constant for NO binding to the Fe^{II}-(TPP) in toluene was found to be 5.2×10^9 M^{-1} s^{-1} at 25 °C).[23] This means that, in the studied case, $k_a \ll k_{-D}$, and the k_{on} expression can be simplified to eq 7.

$$k_{on} = k_a k_D/k_{-D} \quad (7)$$

For the activation-limited process, the activation parameters for the "on" reaction can be defined as follows:

$$\Delta H^{\ddagger}_{on} = \Delta H^{\ddagger}(k_a) + \Delta H^{\ddagger}(k_D) - \Delta H^{\ddagger}(k_{-D}) = \\ \Delta H^{\ddagger}(k_a) + \Delta H^{\circ}(K_D) \quad (8)$$

$$\Delta S^{\ddagger}_{on} = \Delta S^{\ddagger}(k_a) + \Delta S^{\ddagger}(k_D) - \Delta S^{\ddagger}(k_{-D}) = \\ \Delta S^{\ddagger}(k_a) + \Delta S^{\circ}(K_D) \quad (9)$$

$$\Delta V^{\ddagger}_{on} = \Delta V^{\ddagger}(k_a) + \Delta V^{\ddagger}(k_D) - \Delta V^{\ddagger}(k_{-D}) = \\ \Delta V^{\ddagger}(k_a) + \Delta V^{\circ}(K_D) \quad (10)$$

Thus, the values of the apparent activation parameters ($\Delta H^{\ddagger}_{on}$, $\Delta S^{\ddagger}_{on}$) for k_{on} are the sum of two terms, viz. activation enthalpy or entropy for the activation step (k_a) and reaction enthalpy or entropy for the encounter complex formation (K_D). The k_{on} values determined in the present study seem to be little influenced by temperature. The activation parameters for the formation of the nitrosyl complex of **2** show a good agreement between measurements made by using low-temperature stopped-flow and laser flash photolysis techniques and are characterized by a very small value of $\Delta H^{\ddagger}_{on}$ and a substantially large and negative value of $\Delta S^{\ddagger}_{on}$. Since the overall reaction is an exothermic process, it is reasonable to expect that the reaction enthalpy for the encounter complex formation ($\Delta H^{\circ}(K_D)$) will also give a negative contribution to the expression for $\Delta H^{\ddagger}_{on}$ and lead to partial compensation of the two opposite terms. In such a case, the sum of $\Delta H^{\ddagger}(k_a)$ and $\Delta H^{\circ}(K_D)$, represented by eq 8, would be a small value.

It should be noted that the negative values found for the activation entropy and activation volume are also consistent with an activation-controlled reaction mechanism, i.e., rate-determining Fe^{III}—NO bond formation. Moreover, the substantially negative values can be partially associated with a spin change from high-spin Fe(III) (sextet **2** complex, $S = 5/2$ plus doublet NO, $S = 1/2$) to low-spin Fe^{III}—NO (singlet **2**(NO), $S = 0$) during

the binding of NO. As revealed by the EPR measurements, the **2**(NO) complex in toluene appears to be EPR silent, indicating that **2**(NO) is formally a Fe^{II}—NO$^+$ species. A similar behavior was observed for many nitrosyl complexes of ferric hemoproteins or synthetic Fe(III) porphyrins.[23] The appearance of the weak "unusual" EPR signal with characteristic shape and g value ($g = 1.98$) can be ascribed to nonspecific interactions of excess NO with the matrix or other trace contaminant present in the NO-saturated solution. Indeed, this feature has been observed by others,[24] and it was confirmed in the present study that the anomalous resonance at $g = 1.98$ (or 1.99) was reproducible in concentrated NO solutions alone. Furthermore, in our investigation, complete reversibility of the nitrosylation reaction of **2** in toluene was obtained. After removal of NO from the EPR sample of **2**(NO) in toluene, complete recovery of the signal at $g = 5.78$ was observed, indicating complete re-formation of the high-spin complex **2**. Hence, the unusual EPR signal did not originate from the interaction of NO with the reduced form of complex **2**, i.e., via reductive nitrosylation,[23c] but from NO itself.

It is very likely that the spin-state change during the nitrosylation process can account for the relatively small values of the NO binding rate constants (k_{on}) found in the present study in comparison to the rates found for the reaction of NO with five-coordinate ferrous heme proteins or other synthetic porphyrins which also have a vacant coordination site as in **2**. As already shown by Hoshino and Kogure[25] for a series of model porphyrin complexes, the smallest NO binding rate constants were found for complexes that have to undergo the largest reorganization in terms of spin multiplicity. For example, the rate of NO binding to Mn^{II}TPP (high-spin Mn^{II}TPP, $S = 5/2$, after NO binding gives low-spin Mn^{II}TPP(NO), $S = 0$) was almost 2 orders of magnitude slower than the reaction of NO with Fe^{II}TPP (high-spin Fe^{II}TPP, $S = 2$, after NO binding gives low-spin Fe^{II}TPP(NO), $S = 1/2$) and Co^{II}TPP (low-spin Co^{II}-TPP, $S = 1/2$, after NO binding gives low-spin Co^{II}TPP(NO), $S = 0$). In the present system, binding of NO to Fe(III) is accompanied by a large spin change from $S = 5/2$ to $S = 0$. Moreover, IR spectroscopy revealed that the ν_{N-O} mode in **2**(NO) ($\nu_{N-O} = 1833$ cm^{-1}) is close in its nature to the ν_{N-O} modes of other natural heme—thiolate-containing enzymes.[17,18] This suggests that the Fe—NO group in the nitrosyl complex of **2** also adopts a linear structure and formally can be described as Fe^{II}—NO$^+$, as observed, for example, in P450$_{cam}$(NO).[26] This means that Fe^{III}—NO bond formation in the k_a pathway (eq 5) should be accompanied by considerable charge transfer from NO to the Fe(III) center to formally give Fe^{II}—NO$^+$.

The activation parameters ($\Delta H^{\ddagger}_{off}$, $\Delta S^{\ddagger}_{off}$, and $\Delta V^{\ddagger}_{off}$) for the release of NO from the nitrosyl complex of **2** are consistent with a reaction mechanism in which the iron—nitrosyl bond is broken. During this process, the spin state of iron changes from low-spin to high-spin, which will result in a positive contribution to the values of $\Delta S^{\ddagger}_{off}$ and $\Delta V^{\ddagger}_{off}$. Since in the complex **2**(NO), Fe^{III}—NO has Fe^{II}—NO$^+$ character, Fe—NO bond cleavage

(23) (a) Ebel, R. E.; O'Keeffe, D. H.; Peterson, J. A. *FEBS Lett.* **1975**, *55*, 198. (b) O'Keeffe, D. H.; Ebel, R. E.; Peterson, J. A. *J. Biol. Chem.* **1978**, *253*, 3509. (c) Yonetani, T.; Yamamoto, H.; Erman, J. E.; Leigh, J. S., Jr.; Reed, G. H. *J. Biol. Chem.* **1972**, *247*, 2447.

(24) (a) Nelson, M. J. *J. Biol. Chem.* **1987**, *262*, 12137. (b) Arciero, D. M.; Orville, A. M.; Lipscomb, J. D. *J. Biol. Chem.* **1985**, *260*, 14035. (c) Brouwer, M.; Chamulitrat, W.; Ferruzzi, G.; Sauls, D. L.; Weinberg, J. B. *Blood* **1996**, *88*, 1857. (d) Wolak, M.; Stochel, G.; Hamza, M.; van Eldik, R. *Inorg. Chem.* **2000**, *39*, 2018.

(25) Hoshino, M.; Kogure, M. *J. Phys. Chem.* **1989**, *93*, 5478.

(26) Hu, S.; Kincaid, J. R. *J. Am. Chem. Soc.* **1991**, *113*, 2843.

Table 6. Comparison of the Rate and Equilibrium Constants and Thermodynamic and Kinetic Parameters for NO Binding to the Five-Coordinate High-Spin Iron(III) Center in P450$_{cam}$ (Camphor-Bound Form)[12] and Complex **2** in Toluene

	P450$_{cam}$ + camphor (E·S-P450$_{cam}$)[12]	complex **2** in toluene
k_{on} (M^{-1} s^{-1}) at 25 °C	$(3.2 \pm 0.5) \times 10^6$	$(1.80 \pm 0.05) \times 10^6$
$\Delta H^{\ddagger}_{on}$ (kJ mol^{-1})	14. 1 $\pm$ 0.1	4 $\pm$ 2
$\Delta S^{\ddagger}_{on}$ (J mol^{-1} K^{-1})	-73.1 ± 0.4	-111 ± 6
$\Delta G^{\ddagger}_{on}$ (kJ mol^{-1}) at 25 °C	35.9 $\pm$ 0.1	37 $\pm$ 2
$\Delta V^{\ddagger}_{on}$ (cm^3 mol^{-1})	-7.3 ± 0.2	-25 ± 1
k_{off} (s^{-1}) at 25 °C	1.93 $\pm$ 0.02	$(1.25 \pm 0.01) \times 10^4$
$\Delta H^{\ddagger}_{off}$ (kJ mol^{-1})	83.8 $\pm$ 0.7	58 $\pm$ 1
$\Delta S^{\ddagger}_{off}$ (J mol^{-1} K^{-1})	$+41 \pm 2$	$+29 \pm 5$
$\Delta G^{\ddagger}_{off}$ (kJ mol^{-1}) at 25 °C	71.6 $\pm$ 0.7	50 $\pm$ 1
$\Delta V^{\ddagger}_{off}$ (cm^3 mol^{-1})	$+24 \pm 1$	$+7 \pm 3$
K_{NO} (M^{-1}) at 25 °C	$(1.2 \pm 0.4) \times 10^6$	122 $\pm$ 10
ΔH° (kJ mol^{-1})	-69.7 ± 0.8	-71 ± 3
ΔS° (J mol^{-1} K^{-1})	-114 ± 2	-197 ± 10
ΔH° (kJ mol^{-1}) at 25 °C	-35.7 ± 0.7	-12 ± 3
ΔV° (cm^3 mol^{-1})	-31.3 ± 1.2	-39 ± 2

should formally be accompanied by charge transfer from the metal to the nitrosyl ligand, i.e., a formal oxidation of Fe^{II} to Fe^{III}.

Complex 2 as a Model for Cytochrome P450. The five-coordinate, high-spin Fe(III) porphyrin **2** in a non-coordinating solvent such as toluene can be regarded as an analogue of the E·S complex of cytochrome P450$_{cam}$, having the same coordination sphere except for the replacement of a H-bonded thiolate ligand in the enzyme by a SO$_3^-$ ligand in **2**. This difference does not seem to influence the second-order rate constant k_{on} significantly. As shown in Table 6, k_{on} for E·S-P450$_{cam}$ is only 1.8 times higher than k_{on} for binding NO to **2**, and hence it seems that, in both cases, k_{on} is dominated by spin-state changes from high-spin to low-spin on binding of NO. The major differences between **2** and E·S-P450$_{cam}$, however, are (i) the protein environment and (ii) the presence of (+)-camphor bound at the distal side at a distance of 4 Å from the CH$_2$ group (C-5 of the substrate) to Fe(III). Accordingly, there is free access for NO to bind to Fe(III) of **2** but considerable hindrance of camphor for binding NO to Fe(III) of protoporphyrin IX. This is expected to be reflected in the different activation parameters for the "on" reaction of **2** versus E·S-P450$_{cam}$.

The value of the activation enthalpy determined for the reaction between NO and **2** was found to be much lower than for the E·S-P450$_{cam}$/NO system. It is accompanied by much more negative values for the activation entropy and activation volume compared to those reported for NO binding to E·S-P450$_{cam}$ (see Table 6). In contrast, the rate constant for NO dissociation from the nitrosyl complex of **2** is almost 4 orders of magnitude larger than the corresponding k_{off} value obtained for the E·S-P450$_{cam}$/NO system (see Table 6). It has already been shown that NO dissociation rates for Fe(Por)(NO) systems are largely affected by the nature of the binding site. For example, coordination of the proximal histidine to the iron(II) of sGC reduces the equilibrium constant for NO binding by a factor of 10^4, with most of the decrease being due to a dramatic increase in NO dissociation rate.[27] Similarly, changing the features of the porphyrin ligand in a series of Fe^{III}(Por)(NO) complexes, where Por = TMPS, TPPS, and TMPyP, tunes the

k_{off} values from $(0.9 \pm 0.2) \times 10^3$ to $(0.5 \pm 0.2) \times 10^3$ and 28.8 $\pm$ 0.8 s^{-1}, respectively.[22,28] The extremely large value of k_{off} found for the dissociation of NO from **2**(NO) can also be accounted for in a similar way. It seems likely that, in this case, the electron-donating character of the fifth ligand (RSO$_3^-$ group) plays an important role.

It is important to note that k_{off} values obtained for NO dissociation from nitrosyl complexes of model Fe(III) porphyrins are in general much larger than the corresponding k_{off} values found for nitrosyl complexes of native iron(III) hemoproteins.[29,30] Considering the release of NO from the nitrosyl complex of E·S-P450$_{cam}$, at least two factors are expected to dominate the NO dissociation/mechanism: (i) the electron-donating character of the thiolate-H-bonded proximal ligand and (ii) the interaction of the iron(III)-bonded NO with camphor or with the protein active site. It is reasonable that these factors will contribute to the significantly more positive values of the activation parameters found for NO dissociation from the nitrosyl complex of camphor-bound P450$_{cam}$ compared to those found for the **2**(NO) system.

As a result of the high value of k_{off} for the **2**(NO) complex, the equilibrium constant K_{NO}^{tol} for NO binding to complex **2** in toluene appears to be 4 orders of magnitude smaller than K_{NO} found for the reaction between NO and E·S-P450$_{cam}$ (Table 6). The overall reaction volumes seem to be similar for the E·S-P450$_{cam}$/NO and **2**/NO systems and indicate a drastic volume decrease on going from the reactant to the product states, which can be partially ascribed to the high-spin ($S = {}^5/_2$) to low-spin ($S = 0$) transition of the Fe(III) center during the binding of NO. However, despite the similarity in the ΔV° values, the volume profile in terms of the position of the transition state for the reaction between NO and camphor-bound P450$_{cam}$ differs significantly from that observed for the binding of NO to complex **2** in toluene. As can be seen from Figure 9b, in the case of NO binding to E·S-P450$_{cam}$ the transition state for the "on" reaction can be described as "early" and that for the "off" reaction as "late" in terms of the overall volume change during the reaction; i.e., the nature of the transition state is close to that of the reactant state. This trend also corresponds to a relatively fast "on" and a slow "off" reaction and the resulting high binding constant for NO. In the transition state, the NO molecule seems to be only partially bound to E·S-P450$_{cam}$. Following the transition state, there is a large volume collapse associated with the completion of bond formation and the high-to-low spin change. A different scenario is observed for the reaction between NO and **2**. In this case, the volume profile (Figure 9a) clearly demonstrates a "late" transition state for the "on" reaction and an "early" transition state for the "off" reaction, which is in agreement with relatively slow "on" and fast "off" reactions and the resulting much lower binding constant for NO. Furthermore, the activation volume for the binding of NO is significantly negative. This volume collapse is close to the partial molar volume of NO that has been reported to be 27 cm^3 mol^{-1} in aqueous solution at 25 °C.[31] This suggests that the volume collapse associated with the forward reaction

(27) Sharma, V. S.; Magde, D. *Methods—Companion to Methods Enzymol.* **1999**, *19*, 494.

(28) Theodoridis, A.; van Eldik, R. *J. Mol. Catal. A: Chem.* **2004**, *224*, 197.
(29) Hoshino, M.; Laverman, L. E.; Ford, P. C. *Coord. Chem. Rev.* **1999**, *187*, 75 and references cited therein.
(30) Wanat, A.; Wolak, M.; Orzel, l.; Brindell, M.; van Eldik, R.; Stochel, G. *Coord. Chem. Rev.* **2002**, *229*, 37 and references cited therein.
(31) Plyasunov, A. V.; O'Connell, J. P.; Wood, R. H. *Geochim. Cosmochim. Acta* **2000**, *64*, 495.

a)

b)
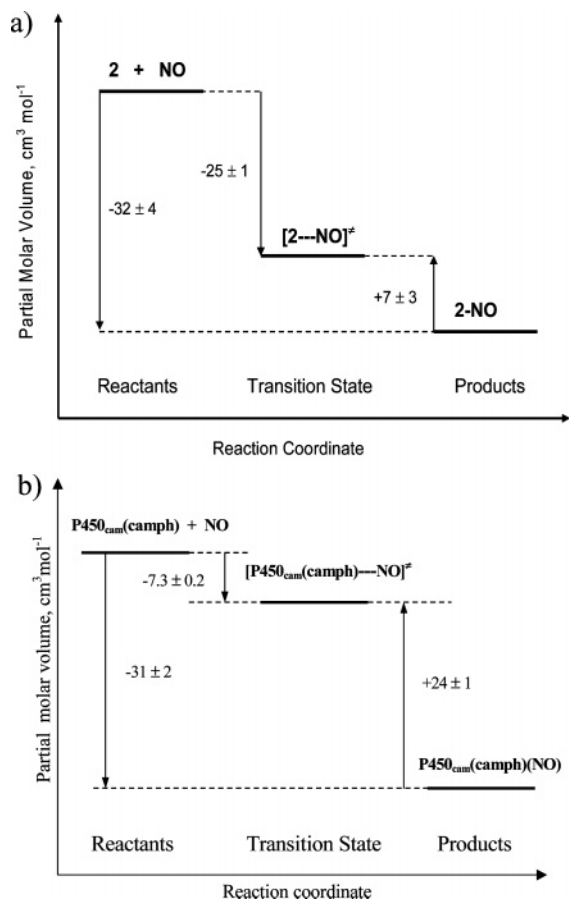
Figure 9. Comparison of volume profiles for NO binding to (a) complex **2** in toluene and (b) camphor-bound P450$_{cam}$.[13]

is prevalently due to the entry of NO into coordination sphere and formation of the Fe−NO bond. Since the high-spin → low-spin transformation is accompanied by a volume decrease of between 12 and 15 cm^3 mol^{-1},[32] the subsequent volume collapse of 7 ± 3 cm^3 mol^{-1} following the transition state can be ascribed to the spin-state change on the Fe center. A similar behavior was observed in the case of binding of carbon monoxide to the iron(II) cyclidene complex [Fe^{II}(PhBzXy)](PF$_6$)$_2$.[33] The volume profile found for this reaction clearly shows a "late" transition state in terms of Fe−CO bond formation, corresponding mainly to the volume change associated with the disappearance of the CO molecule into the ligand pocket (volume collapse $\sim$37 cm^3 mol^{-1} in toluene). Following the transition state, there is a high-spin to low-spin change on the iron(II) center, during which the metal center moves into the ligand plane (volume collapse $\sim$11 cm^3 mol^{-1}).

Suggested Mechanism for Formation of 2(NO) in Methanol. The spectrum of complex **5** in methanol displays a characteristic split Soret band which is indicative of the six-coordinate Fe(III) porphyrin **5**. Such a behavior is predicted by calculation for six-coordinate heme−thiolate systems.[34] The small value of the formation constant found for the binding of methanol to complex **2** ($K_{MeOH} = 0.20 \pm 0.05$ M^{-1} at 25 °C) suggests that CH$_3$OH must be weakly bound to the Fe(III)

(32) (a) Messana, C.; Cerdonio, M.; Shenkin, P.; Noble, R.; Fermi, G.; Perutz, R. N.; Perutz, M. F. *Biochemistry* **1978**, *17*, 3652. (b) Morishima, L.; Ogawa, S.; Yamada, H. *Biochemistry* **1980**, *19*, 1569.
(33) Buchalova, M.; Busch, D. H.; van Eldik, R. *Inorg. Chem.* **1998**, *37*, 1116.
(34) Loew, G. *Int. J. Quantum Chem.* **2000**, *77*, 54.

center. As shown by EPR measurements, this interaction does not lead to a change in the spin state of Fe(III), and complex **5** remains a high-spin species in methanol. The relatively small values of the thermodynamic parameters, especially the reaction volume ($\Delta V° = -6.5 \pm 0.2$ cm^3 mol^{-1}), found for equilibrium (3) also confirm this observation. They are characteristic for the binding of methanol to the Fe(III) center of **2** without a change in the spin state of the metal.

The reaction between NO and **5** in methanol is almost 300 times slower (at −70 °C) than that in toluene. This can be ascribed to the vacant position in the coordination sphere of complex **2** in toluene, which is a non-coordinating solvent. In methanol, the coordination site is occupied by a methanol molecule that is H-bonded to MeOH solvent molecules (see **5**), which must be displaced by NO. A similar scenario was observed in the case of NO binding to the heme−thiolate model complex **4** in methanol, which was almost 3 orders of magnitude slower than the reaction in toluene.[13] The overall reaction volume found for NO binding to **2** is more positive (of about $6-10$ cm^3 mol^{-1}) than that found in toluene. Since the overall reaction for the association of MeOH with complex **2** in toluene is accompanied by a volume collapse of 6.5 ± 0.1 cm^3 mol^{-1}, it is reasonable to conclude that the difference between the $\Delta V°$ values for the nitrosylation reactions of **2** in toluene and **5** in MeOH is mainly due to displacement of a methanol molecule from the coordination sphere of iron(III) in the latter case. All these observations, along with the small value of ΔH and substantially negative value of ΔS found for NO binding to **5**, are consistent with an associative interchange (I$_a$) mechanism, as expressed in eq 11.


$$(11)$$
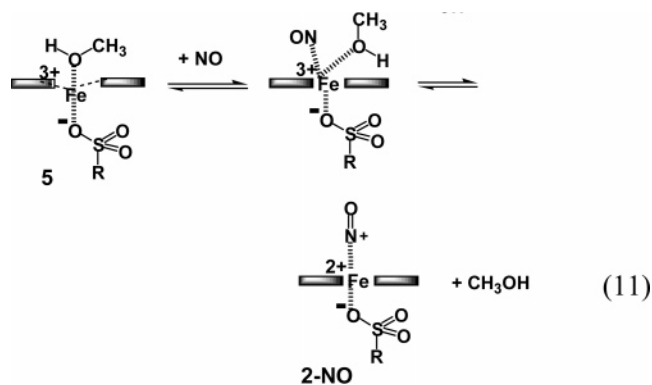
As a result, the value of $\Delta H^{\ddagger}_{on}{}^{met}$ reported in this study for the forward reaction must include the energy required to partially break the Fe^{III}−CH$_3$OH bond and should therefore be much larger than the corresponding value determined in a non-coordinating solvent. In such a case, the activation entropy, $\Delta S^{\ddagger}_{on}{}^{met}$, involves a positive contribution from the partial cleavage of the Fe^{III}−CH$_3$OH bond and should be significantly more positive than the corresponding value found in toluene. Similarly, the value of the activation volume for NO binding to **5** in methanol, $\Delta V^{\ddagger}_{on}{}^{met}$, is also expected to be more positive than the value of $\Delta V^{\ddagger}_{on}$ found in toluene. However, due to the instability of the nitrosyl complex in methanol (a subsequent, slow reaction was observed following NO binding to **5**), we were not able to determine $\Delta V^{\ddagger}_{on}{}^{met}$ in methanol with the laser flash photolysis technique. Furthermore, the NO binding reaction was too fast for the high-pressure stopped-flow technique. It is

a)

b)
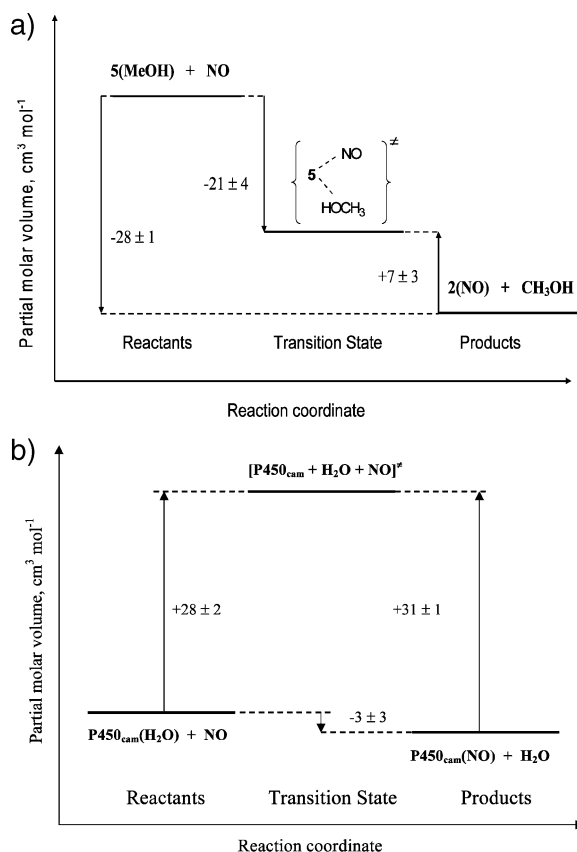
Figure 10. Volume profiles for reversible NO binding to (a) complex **5** in methanol and (b) the substrate-free form of P450$_{cam}$.

	P450$_{cam}$ resting state[12]	complex **5** in methanol
k_{on} (M^{-1} s^{-1}) at 25 °C	$(3.20 \pm 0.02) \times 10^5$	$(0.6 \pm 0.05) \times 10^{5\ a}$
$\Delta H^{\ddagger}_{on}$ (kJ mol^{-1})	92 ± 1	14 ± 1
$\Delta S^{\ddagger}_{on}$ (J mol^{-1} K^{-1})	$+169 \pm 4$	-107 ± 3
$\Delta G^{\ddagger}_{on}$ (kJ mol^{-1}) at 25 °C	42 ± 1	46 ± 1
$\Delta V^{\ddagger}_{on}$ (cm^3 mol^{-1})	$+28 \pm 2$	-21 ± 4^{b}
k_{off} (s^{-1}) at 25 °C	0.35 ± 0.02	2249 ± 167^{c}
$\Delta H^{\ddagger}_{off}$ (kJ mol^{-1})	122 ± 4	44 ± 5
$\Delta S^{\ddagger}_{off}$ (J mol^{-1} K^{-1})	$+155 \pm 15$	-34 ± 22
$\Delta G^{\ddagger}_{off}$ (kJ mol^{-1}) at 25 °C	76 ± 4	54 ± 5
$\Delta V^{\ddagger}_{off}$ (cm^3 mol^{-1})	$+31 \pm 1$	$+7 \pm 3^{d}$
K_{NO} (M^{-1}) at 25 °C	$(9.0 \pm 0.2) \times 10^5$	27 ± 3
ΔH° (kJ mol^{-1})	-30 ± 5	-59 ± 4
ΔS° (J mol^{-1} K^{-1})	$+14 \pm 19$	-169 ± 13
ΔG° (kJ mol^{-1}) at 25 °C	-34 ± 4	-9 ± 4
ΔV° (cm^3 mol^{-1})	$+3 \pm 3$	-28 ± 1

^{a} Value extrapolated from the Eyring plot of $\ln(k_{on}/T)$ vs $1/T$. ^{b} Value estimated from $\Delta V^{\circ}_{NO}{}^{met} - \Delta V^{\ddagger}_{off}{}^{met}$. ^{c} Value extrapolated from the Eyring plot of $\ln(k_{off}/T)$ vs $1/T$. ^{d} Value determined in toluene (see text).

reasonable to expect that the volume collapse ascribed to the high-spin → low-spin change on the iron(III) center during the binding of NO to **5** in methanol should be very close to that determined for the nitrosylation reaction in toluene, i.e., ~7 ± 3 cm^3 mol^{-1}. Since the overall binding of NO to **5** in methanol was accompanied by a volume collapse of 28 cm^3 mol^{-1}, the volume change associated with Fe^{III}−NO bond formation and Fe^{III}−CH$_3$OH bond cleavage can be estimated to be −21 cm^3 mol^{-1}. On the assumption that the transition state in this case can also be described as "late" (as observed for the reaction in toluene), the value of $\Delta V^{\ddagger}_{on}{}^{met}$ for the forward reaction (eq 4) is expected to be about −21 cm^3 mol^{-1}. This value is significantly more positive than the corresponding value found for the nitrosylation reaction in toluene, which is associated with the displacement of the coordinated methanol molecule from the iron(III) center. The volume profile for the reversible binding of NO to complex **5** in methanol, constructed on the basis of these extrapolated data, is shown in Figure 10a.

The activation parameters for the release of NO from **2**(NO) in methanol, determined from the plot of k_{obs} vs [NO], are characterized by a relatively small value of $\Delta H^{\ddagger}_{off}{}^{met}$ and a negative value of $\Delta S^{\ddagger}_{off}{}^{met}$. In principle, in terms of microscopic reversibility, the reverse process (k_{off} pathway) must proceed via the same transition state as that generated during the k_{on} pathway and should also follow an associative interchange mechanism. This seems to contradict the significantly positive value found for $\Delta V^{\ddagger}_{off}{}^{met}$. However, the "off" reaction is controlled by a change in spin state from low-spin to high-spin, which results in a significant volume increase on going to the

transition state that offsets the volume collapse expected for the binding of methanol in terms of an associative interchange mechanism.

Substitution Behavior of Complex 5 and the Resting State of P450$_{cam}$ in Their Reactions with NO. The resting state of P450$_{cam}$ is predominantly a low-spin ($S = {}^1/_2$), six-coordinate complex with one water molecule of a water cluster bound to Fe(III) at the distal site. A similar coordination environment of the Fe(III) center is observed for complex **5** in methanol. However, the significant difference between these two complexes is the Fe(III) spin state. As already mentioned, after coordination of methanol, complex **2** remains in the high-spin state. The value of the NO binding rate constant determined for **5** in methanol at 25 °C is a little lower than that found for the reaction between NO and substrate-free P450$_{cam}$ (Table 7). The activation parameters found for both "on" and "off" reactions seem to be totally different, and they are significantly more positive in the case of the reaction between NO and P450$_{cam}$.

For the mechanistic interpretation of NO binding to substrate-free P450$_{cam}$, a dissociative ligand substitution mechanism was proposed. Accordingly, the activation parameters $\Delta S^{\ddagger}_{on}$ and $\Delta V^{\ddagger}_{on}$ for the reaction between substrate-free P450$_{cam}$ and NO were found to be dominated by dissociation of a water molecule from P450$_{cam}$(H$_2$O) to form the five-coordinate, high-spin intermediate. A different scenario is observed for the reaction between complex **5** and NO. In this case, these activation parameters are more negative and clearly support an associative interchange mechanism with a relatively strong contribution from the entering NO molecule. Notably, the factors that can, to a large extent, contribute to the more positive values of the activation parameters found for the reaction between NO and the resting state of P450$_{cam}$ compared to the values for the related reaction with complex **5** in methanol may be associated with the presence of water molecules in the protein coat. The resulting Fe^{II}−NO$^+$ complex can be stabilized by H-bonding and Coulomb interaction with the water molecules that remain in the vicinity of the Fe−NO bond. Regarding the nitrosyl complex in methanol, there is also stabilization of the Fe−NO bond by

H-bonding and Coulomb interactions to the solvent molecules, but these should be less rigidly organized since it concerns the distal site of the resting state of P450$_{cam}$. Therefore, it is reasonable to expect that the dissociation of NO from the P450$_{cam}$−NO complex should be much slower than in the case of NO release from model complex **2**(NO) in methanol and accompanied by more positive values of the mentioned activation parameters.

As can be expected, the very large value of k_{off} for **2**(NO) in methanol significantly reduces the equilibrium constant for NO binding to $K_{NO}^{met} = 27$ M^{-1}, which is several orders of magnitude lower than K_{NO} found for the reaction between NO and substrate-free P450$_{cam}$ (see Table 7). The reaction enthalpies for both reactions appear to be significantly negative, with $\Delta H°$ for NO binding to **5** almost 2 times more negative than for the P450$_{cam}$−NO system. The entropy and volume changes for the overall **5** + NO reaction in methanol do not correlate well with the corresponding reaction parameters obtained for NO binding to substrate-free P450$_{cam}$. For the reaction between NO and complex **5** in methanol, a drastic volume decrease on going from the reactant to the product state can be observed (Figure 10a), while the overall volume change associated with NO binding to the resting state of P450$_{cam}$ is close to zero (Figure 10b). This difference can be directly related with the change in spin state during the reaction. In the case of the resting state of P450$_{cam}$, there is no major change in spin state on going from the reactant to the product state since both complexes are in the low-spin state. However, complex **5** in methanol is in the high-spin change, which changes to the low-spin state accompanied by a large volume collapse on binding NO.

Conclusions

We have demonstrated herein that, although the model complex **2** lacks protein architecture and possesses a SO$_3^-$ group as proximal ligand, it displays NO binding rate constants in a non-coordinating solvent that are very close to those measured for the "on" reaction between NO and native E·S-P450$_{cam}$. In contrast, the rate constants for NO dissociation from the nitrosyl adducts of **2** and E·S-P450$_{cam}$ differ by almost 4 orders of magnitude, which accounts for the much lower NO binding constant of **2**. On the basis of the activation parameters found for NO binding to the model complex **2** and E·S-P450$_{cam}$, it can be concluded that both reactions follow the same mechanism, which is dominated by Fe^{III}−NO bond formation with a concomitant change in the iron(III) spin state (from $S = {}^5/_2$ to $S = 0$). However, despite this similarity, the volume profiles for NO binding to **2** and E·S-P450$_{cam}$ clearly indicate that the transition states for these reactions differ significantly in terms of contributions arising from bond formation and change in spin state.

Kinetic experiments carried out in a coordinating solvent can reflect the importance of the iron(III) coordination mode in terms of a sixth distal ligand in substitution reactions with NO. We have demonstrated that the presence of methanol coordinated to the iron(III) center slows down the binding of NO to complex **5** ca. 10 times (at 25 °C) compared to the same reaction with complex **2**, which lacks the sixth ligand. It should be noted that a similar behavior was observed for the binding of NO to ferric P450$_{cam}$ in the absence (six-coordinate P450$_{cam}$) and in the presence (five-coordinate P450$_{cam}$) of camphor as substrate.[12]

The rate constants for the "on" and "off" reactions in methanol show the same trends as those measured for the reactions in toluene (compare Tables 6 and 7). However, the activation parameters for the reversible binding of NO to the resting state of P450$_{cam}$ and **5** in methanol differ significantly. Whereas the dissociation of a coordinated water molecule coupled to a high-spin to low-spin change controls the binding of NO to P450$_{cam}$, the displacement of weakly coordinated methanol on **5** follows an associative interchange process in which the volume collapse results from bond formation and a change from high-spin to low-spin. The resting state of P450$_{cam}$ is a low-spin state, whereas our EPR measurements clearly indicated that complex **5** in methanol is in a high-spin state. These opposite effects are clearly illustrated by the volume profiles for these processes (see Figure 10).

Both complexes **2** and **5** bind NO ca. 4 orders of magnitude more weakly than P450$_{cam}$ at 25 °C, which can be accounted for in terms of a very effective "off" reaction. However, at low temperature, the binding constants increase significantly due to the exothermic nature of the binding process and a much slower "off" reaction. The data for the model complex clearly highlight the unique behavior of the P450 enzyme, in that the enzyme binds NO much more strongly at room temperature than the model complex. This must be related to the role played by the enzyme pocket, which stabilizes the formation of the NO$^+$ state. This is a general observation made with model enzymes that mimic, for instance, the binding of dioxygen to hemeocyanine and tyrosinase, for which much lower temperatures are required to stabilize intermediate oxidant or substrate-bound species. Thus, the unique structure of the protein pocket must be responsible for the high binding constants at ambient temperature as compared to those observed for many model complexes that do not exhibit these unique features.

The present results, along with our previous studies,[12,13] demonstrate that, as in biological systems, ligand substitution behavior of synthetic iron(III) porphyrin complexes can be regulated by tuning the electronic nature of the porphyrin (introduction of electron-withdrawing/donating substituents on the porphyrin ring), the electronic nature of the axial ligands (for example, replacement of the strong electron-donating ligands with less electron-rich groups, RS$^-$ → RSO$_3^-$), and experimental conditions such as the selected solvent (coordinating vs non-coordinating) and pH (deprotonation of coordinating protic solvents). Therefore, the results of this study lay the basis for further investigations on the catalytic activity of complexes **2** and **5** in the activation of peroxides for the oxidation/hydroxylation of suitable substrate molecules.

Supporting Information Available: Figure S1, EPR spectrum of a degassed toluene solution saturated with NO; Figure S2, plots of k_{obs} as a function of [NO] for NO binding to **2**; Figure S3, plots of k_{obs} versus [NO] as a function of temperature for

NO binding to **2** measured by laser flash photolysis; Figure S4, plots of ln(k) versus pressure for the "on" and "off" reactions for the reversible binding of NO to complex **2** measured by laser flash photolysis; Figure S5, spectral changes recorded during titration of **2** in toluene with methanol (inset: plot of (ΔAbs)$^{-1}$ vs [MeOH]$^{-1}$ to determine the equilibrium constant for reaction (3)); Figure S6, plots of ln(K_{MeOH}) vs (a) $1/T$ and (b) pressure for methanol binding to complex **2** in toluene; Figure S7, EPR spectra of (a) complex **2** in MeOH/toluene and (b) complex **2** in MeOK–MeOH/toluene; Figure S8, spectral changes for the reaction between **5** and NO in methanol as a function of (a) temperature and (b) pressure; Figure S9, spectral

changes recorded during NO binding to **5** in methanol (inset: typical absorbance–time plot for NO binding to **5**); Figure S10, plots of k_{obs} as a function of [NO] for NO binding to **5** in methanol; Figure S11, spectra recorded for the subsequent slow reaction in methanol; and Figure S12, absorption spectra recorded for **5** (line 1) after reduction with NaBH$_4$ (line 2) and following the reaction with NO (line 3) in methanol. This material is available free of charge via the Internet at http://pubs.acs.org.

JA060650O